The current issue and full text archive of this journal is available at
http://www.emerald-library.com

Computational modeling of a dilute turbulent liquid-solid flow using a Eulerian-Lagrangian approach

X.-Q. Chen
University of Waterloo, Waterloo, Ontario, Canada and
J.C.F. Pereira
Department of Mechanical Engineering, Instituto Superior Tecnico/ Technical University of Lisbon, Lisbon, Portugal

Received September 1999
Revised February 2000
Accepted February 2000

Keywords *Computational model, Numerical methods, Flow*

Abstract *Numerical results are reported for a dilute turbulent liquid-solid flow in an axisymmetric sudden-expansion pipe with an expansion ratio 2:1. The two-phase flow has a mass-loading ratio low enough for particle collision to be negligible. The numerical predictions for the dilute two-phase flow are based on a hybrid Eulerian-Lagrangian model. A nonlinear* k-ε *model is used for the fluid flow to account for the turbulence anisotropy and an improved eddy-interaction model is used for the particulate flow to account for the effects of turbulence anisotropy, turbulence inhomogeneity, particle drift, and particle inertia on particle dispersion. The effects of the coupling sources, the added mass, the lift force and the shear stress on two-phase flow predictions are separately studied. The numerical predictions obtained with the improved and conventional particle dispersion models are compared with experimental measurements for the mean and fluctuating velocities at the different measured planes.*

Nomenclature

D_{pi} = particle diameter of size i
f_p = drag correction efficient (= 1 + 0.15 $\mathrm{Re}_p^{0.687}$)
g = gravitational force
N = number flow rate
P = pressure
r = radial distance from the symmetry axis
RMS = root mean squared
Re_p = relative Reynolds number between the two phases
$S_{u_i}^p$ = momentum source for U_i from the particle phase
S_k^p = turbulence modulation from the particle phase
t = time
τ_p = relaxation time (τ_p^*/f_p)
U = fluid or particle velocity
$\overline{u_i u_j}$ = Reynolds stresses
V_{rel} = relative velocity between the two phases $\left(V_{rel} = \sqrt{(\tilde{U}_i - U_{pi})^2}\right)$
x = Cartesian coordinates

Greek symbols
δ_{ij} = Kronecker delta (= 1, $i = j$; = 0, $i \neq j$)
μ = fluid viscosity
μ_t = fluid turbulent viscosity (= $\rho C_\mu \frac{k^2}{\varepsilon}$)
μ_{eff} = fluid effective viscosity (= $\mu + \mu_t$)
ρ = fluid or particle density
ζ = random variable

Subscripts
CL = centerline
i, j, k, m, n = coordinate components
p = particle phase

The authors greatly appreciate the suggestions of the two referees to clarify and improve the manuscript.

© MCB University Press, 0961-5539

Introduction

Liquid-solid flows are present in a variety of industrial applications, such as the pneumatic conveying system, hydroelectric engineering where water turbines are operated in silt-laden rivers, and petroleum piping systems, etc. For dilute two-phase flows, a combined Eulerian-Lagrangian model has proven to be an efficient tool for the numerical analysis of a two-phase flow system where there exists a continuous and a particulate phase. Such a hybrid Eulerian-Lagrangian model treats the continuous phase using a Eulerian formulation and the particulate phase using a Lagrangian formulation. The interaction between the two phases is realized via coupling sources to account for exchanges in mass, momentum and energy. Different from the two-fluid model (Daniel and Loraud, 1998) where no particle dispersion induced by carrier-flow turbulence is taken into consideration, the hybrid Eulerian-Lagrangian modeling of turbulent two-phase flows often requires accounting for particle dispersion induced by the fluid turbulence. Such turbulence-induced particle dispersion can be modeled using an eddy-interaction model (Gosman and Ioannides, 1981), hereinafter referred to as GI for abbreviation in the present paper.

The GI model assumes that a discrete heavy particle moving in a turbulent carrier flow encounters a series of turbulent energetic eddies. The particle is interacting with an eddy for a period of time, which is determined as the minimum of the eddy lifetime and the eddy transit time. It has been demonstrated (Chen and Pereira, 1996) that the GI model is essentially an isotropic particle dispersion model; it cannot account for the effects of turbulence anisotropy on particle dispersion. The GI model and its variants have been widely used to predict many dilute turbulent two-phase flows (Adeniji-Fashola and Chen, 1990; Chang and Wu, 1994; Chen *et al.*, 1996). A recent analysis (Graham and James, 1996) has indicated, however, that the GI model cannot account for the possibility that the finite-inertia particles may disperse faster than the fluid particles. This is due to the fact that a constraint imposed by the model has led to an outcome that the finite-inertia particles can never interact with an eddy for a time longer than the fluid particles; as a result, the dispersion of the finite-inertia particle in the longtime limit is underpredicted. Evidently, this is in contrast to the experimental observation that the finite-inertia particles may disperse more than the fluid particles. To overcome this model deficiency, Graham and James (1996) introduced an additional maximum particle-eddy interaction time scale into the original GI model. The maximum time scale is independent of the fluid particle interaction time scale, and can be determined in terms of a given turbulence structure. Such a modified GI model was found (Chen and Pereira, 1998) to improve the numerical predictions for a turbulent gas-particle flow, where the particle-eddy interaction time depends much on the maximum time scale.

It is known that the GI model accounts for particle dispersion using the local turbulent kinetic energy to sample the eddy fluctuating velocities; therefore, it

cannot account for the effects of turbulence anisotropy on particle dispersion for anisotropic turbulent two-phase flows. To account for the effects of turbulence anisotropy on particle dispersion, Chen and Pereira (1996) modified the GI model by using the local Reynolds stresses, instead of the local turbulent kinetic energy, to determine the eddy fluctuating velocities. It was found that such a modification had improved the prediction of particle-dispersion anisotropy. The GI model also assumes that the eddy fluctuating velocities, sampled at the beginning of encounter, are kept unchanged until the end of the particle-eddy interaction time. For inhomogeneous turbulent two-phase flows, this assumption may result in an artificial transfer of turbulence from the region of high intensity to low intensity within an eddy interaction time. To overcome this drawback, MacInnes and Bracco (1992) suggested that the turbulence inhomogeneity be accounted for by using a normalized fluctuating velocity at the beginning of encounter to define a physical scale. The local turbulence intensity is then used to determine the eddy fluctuating velocities at each time step.

Considering the above-mentioned deficiencies of the original GI model, Chen (2000) recently reformulated the eddy-interaction model to account for all of the possible physical phenomena. Such an improved eddy-interaction model was used to predict particle dispersion in a wall-embedded turbulent gaseous jet (Sato *et al.*, 1996). Numerical results were compared with other predictions, showing an improvement in particle flow predictions. The objective of the present work is to further validate the improved particle dispersion model for a particle-laden turbulent liquid flow. Numerical results obtained with the CFD (Computational Fluid Dynamics) analysis were compared with experimental measurements (Founti and Klipfel, 1994). The considered two-phase flow was dilute so that the interparticle collision could be neglected. To assess the improved particle dispersion model, which takes into account the effects of the turbulence anisotropy, turbulence inhomogeneity, particle inertia, and particle drift correction, the numerical results obtained with the original GI model are also used as a reference. The performance of the original and improved GI models is assessed by comparing their numerical predictions with the experimental measurements.

Modeling of the turbulent liquid flow

The turbulent liquid flow is modeled in terms of the partial-differential equations. The coupling effects between the particle and fluid flows are accounted for through additional source terms. The time-averaged transport equations for continuity and momentum can be written tensorially as follows:

$$\frac{\partial \rho U_j}{\partial x_j} = 0 \tag{1}$$

$$\frac{\partial \rho U_j U_i}{\partial x_j} = -\frac{\partial P}{\partial x_i} + \frac{\partial}{\partial x_j}\left[-\rho\overline{u_i u_j} + \mu\left(\frac{\partial U_i}{\partial x_j} + \frac{\partial U_j}{\partial x_i}\right)\right] + S^{p}_{U_i} \tag{2}$$

where $S_{U_i}^{p}$ accounts for exchange in momentum between the fluid and particle flows. The momentum exchange is included here to account for the effects of two-way coupling between the two phases. The Reynolds stresses, $\overline{u_i u_j}$, are modeled in terms of the nonlinear k-ε model as follows:

$$\rho\overline{u_i u_j} = \frac{2}{3}\rho k\delta_{ij} - \mu_t\left(\frac{\partial U_i}{\partial x_j} + \frac{\partial U_j}{\partial x_i}\right) + \rho\overline{\hat{u}_i\hat{u}_j} \tag{3}$$

where $\rho\overline{\hat{u}_i\hat{u}_j}$ represents the nonlinear part of the Reynolds stresses. The nonlinear part of the Reynolds stresses can be written (Lien and Leschziner, 1994) as follows:

$$\overline{\hat{u}_i\hat{u}_j} = \frac{k^3}{\varepsilon^2}\left[C_{\tau 1}\left(\frac{\partial U_i}{\partial x_k}\frac{\partial U_j}{\partial x_k}\right)^{*} + C_{\tau 2}\left(\frac{\partial U_i}{\partial x_k}\frac{\partial U_k}{\partial x_j} + \frac{\partial U_j}{\partial x_k}\frac{\partial U_k}{\partial x_i}\right)^{*} + C_{\tau 3}\left(\frac{\partial U_k}{\partial x_i}\frac{\partial U_k}{\partial x_j}\right)^{*}\right] \tag{4}$$

where the superscript * represents the deviatoric part, defined as

$$\left(\frac{\partial U_i}{\partial x_k}\frac{\partial U_j}{\partial x_k}\right)^{*} = \frac{\partial U_i}{\partial x_k}\frac{\partial U_j}{\partial x_k} - \frac{1}{3}\frac{\partial U_m}{\partial x_n}\frac{\partial U_m}{\partial x_n}\delta_{ij} \tag{5}$$

Similarly, the other deviatoric parts can be defined. The two-dimensional expansion of equation (4) for either planar or axisymmetric flows can be found elsewhere (Chen *et al.*, 1999). It should be noted that recently Apsley and Leschziner (1998) developed a new low-Reynolds-number nonlinear turbulence model, which uses strain-vorticity-dependent coefficients to capture the response to normal straining. However, the coefficient requires being determined by iteration. In the present work, the constant coefficients are used, since the objective here is to study the particle dispersion models.The equations for the turbulent kinetic energy k and its dissipation rate ε are governed, respectively, by

$$\frac{\partial \rho U_j k}{\partial x_j} = \frac{\partial}{\partial x_j}\left(\frac{\mu_{eff}}{\sigma_k}\frac{\partial k}{\partial x_j}\right) + (G - \rho\varepsilon) + S_k^{p} \tag{6}$$

$$\frac{\partial \rho U_j \varepsilon}{\partial x_j} = \frac{\partial}{\partial x_j}\left(\frac{\mu_{eff}}{\sigma_\varepsilon}\frac{\partial \varepsilon}{\partial x_j}\right) + \frac{\varepsilon}{k}(C_{\varepsilon 1}G - C_{\varepsilon 2}\rho\varepsilon) + C_{p\varepsilon}\frac{\varepsilon}{k}S_k^{p} \tag{7}$$

where turbulence generation is given by

$$G = -\rho\overline{u_i u_j}\frac{\partial U_i}{\partial x_j} = G_c - \rho\overline{\hat{u}_i\hat{u}_j}\frac{\partial U_i}{\partial x_j} \tag{8}$$

The conventional production term of the standard k-ε model, G_c, is given by

$$G_c = \mu_t \left(\frac{\partial U_i}{\partial x_j} + \frac{\partial U_j}{\partial x_i} \right) \frac{\partial U_i}{\partial x_j} \tag{9}$$

The turbulence model constants are given as follows: (C_μ, σ_k, σ_ε, $C_{\varepsilon 1}$, $C_{\varepsilon 2}$, $C_{p\varepsilon}$, $C_{\tau 1}$, $C_{\tau 2}$, $C_{\tau 3}$) = (0.09, 1.0, 1.3, 1.45, 1.9, 1.6, 0.041, 0.014, –0.014). To predict correctly the flow-spreading rate for the present axisymmetric sudden-expansion flow, the model coefficients C_μ and $C_{\varepsilon 2}$ are modified (Rodi, 1972) as follows:

$$C_\mu = 0.09 - 0.04f, C_{\varepsilon 2} = 1.9 - 0.0667f \tag{10}$$

where f is a function of the jet width r_{jet}, the centerline velocity U_{CL}, and its axial derivative $\frac{\partial U_{CL}}{\partial x}$ along the centerline; that is

$$f = \left[\frac{r_{jet}}{2U_{CL}} \left(\left| \frac{\partial U_{CL}}{\partial x} \right| - \frac{\partial U_{CL}}{\partial x} \right) \right]^{0.2} \tag{11}$$

The ensuing comparison will show that the numerical predictions incorporating the above modifications are in better agreement with the experimental measurements than those using the conventional constant coefficients.

Modeling of the particulate flow

In the framework of the hybrid Eulerian-Lagrangian approach to modeling dilute two-phase flows, the motion of particles in the fluid flow is governed by the Lagrangian trajectory equations; that is:

$$\begin{aligned} \frac{dU_{pi}}{dt} = {} & \frac{\tilde{U}_i - U_{pi}}{\tau_p^*} \frac{\mathrm{Re}_p C_D}{24} + \left(1 - \frac{\rho}{\rho_p} \right) g_i + \frac{\rho}{2\rho_p} \frac{d}{dt} \left(\tilde{U}_i - U_{pi} \right) \\ & + \frac{3.0884}{\rho_p D_p} \sqrt{\rho \mu \left| \frac{\partial \tilde{U}_j}{\partial x_m} \right|} \left(\tilde{U}_j - U_{pj} \right) \delta_{mi} \left(1 - \delta_{mj} \right) \end{aligned} \tag{12}$$

where each term on the right-hand side denotes, respectively, the drag, gravity, added mass, and lift forces. The added mass accounts for inertia of the fluid, which a particle displaces as it is accelerating. The lift force accounts for the force induced on a particle by a gradient in local carrier-fluid velocity. As illustrated later, however, the added mass and the lift force have negligible effects for the present dilute two-phase flow. The particle relaxation time constant is defined as

$$\tau_p^* = \frac{\rho_p D_p^2}{18\mu} \tag{13}$$

The relative Reynolds number, Re_p, in equation (12) is defined as:

$$\mathrm{Re}_p = \frac{\rho V_{rel} D_p}{\mu} \tag{14}$$

The drag coefficient is determined as follows:

$$C_D = \begin{cases} \frac{24}{\mathrm{Re}_p}\left(1 + 0.15\mathrm{Re}_p^{0.687}\right) = \frac{24}{\mathrm{Re}_p} f_p & \mathrm{Re}_p \leq 1,000 \\ 0.44 & \mathrm{Re}_p > 1,000 \end{cases} \tag{15}$$

The instantaneous fluid velocity $\tilde{U}_i$ is a velocity that is experienced by a particle along its trajectory. Particular attention should be paid to determining this velocity because it is not known a priori; the solution to the time-averaged fluid flow has only provided the mean flow velocity. The instantaneous fluid velocity consists of a mean and a fluctuating part. The mean part is obtained with the time-averaged Eulerian solution whereas the fluctuating part requires a particle dispersion model.

Modeling of turbulence-induced particle dispersion

Dispersion of discrete particles in the turbulent carrier fluid can be modeled using an eddy-interaction (GI) model. The GI model assumes that a particle moving in the turbulent carrier flow encounters a series of turbulent energetic eddies, which are characterized by a turbulent time scale and a turbulent length scale. The particle is interacting with a randomly sampled eddy for a period of time, determined as the minimum of an eddy lifetime and an eddy transit time. The eddy-transit time accounts for the particle trajectory-crossing effect, which usually reduces particle dispersion. However, the eddy-interaction time for heavy particles in the GI model has the drawback that it cannot exceed the fluid particle interaction time (Graham and James, 1996). As a result, heavy particle dispersion can never exceed fluid particle dispersion. In addition, the GI model has several other deficiencies for the prediction of particle dispersion in inhomogeneous, anisotropic turbulent flows. Noting these deficiencies, Chen (2000) modified the original GI model to account for additional physical phenomena encountered in complex two-phase flows. The reformulated eddy-interaction model can be summarized as follows.

Turbulence anisotropy

In the GI model, the local turbulent kinetic energy is used to determine the eddy fluctuating velocities. However, it is found (Chen and Pereira, 1996) that the use

of the local turbulent kinetic energy yields isotropic predictions of particle dispersion. Hence, the turbulence anisotropy of the particulate phase cannot be predicted adequately. In the present work, the local Reynolds stresses are used for sampling the eddy fluctuating velocities; that is, the eddy fluctuating velocity is determined by

$$u_i = \zeta_i \sqrt{\overline{u_i^2}} \quad \text{(no summation over } i\text{)} \tag{16}$$

where ζ_i is a Gaussian random variable having zero mean and unity deviation. The normal stresses are provided by the nonlinear k-ε model predictions. An interpolation is required to determine the values at the particle position because the particle position usually does not coincide with the numerical node used for the finite-volume solution to the fluid flow. Note that the two random variables, ζ_u and ζ_v, for the two velocity components determined in such a way have not accounted for the effects of the shear stress. However, the shear stress can be accounted for (Chen and Pereira, 1992) by correlating the two random variables as follows:

$$\zeta_v' = \zeta_v \sqrt{1 - \rho_{uv}^2} + \rho_{uv} \zeta_u \tag{17}$$

where ζ^u and ζ^v are two Gaussian random variables having zero mean and unity deviation, and the correlation coefficient is defined as:

$$\rho_{uv} = \frac{\overline{uv}}{\sqrt{\overline{u^2}}\sqrt{\overline{v^2}}} \tag{18}$$

Therefore, $\zeta_u^2 \sqrt{\overline{u^2}}$ and $\zeta_v' \sqrt{\overline{v^2}}$ represent the two correlated components of the eddy fluctuating velocity to be used in the particle momentum equations.

Turbulence inhomogeneity

As the GI model assumes that the fluctuating velocities sampled for an eddy are kept unchanged during the particle-eddy interaction time, therefore, it may happen that fluid turbulence is artificially transferred from the region of high intensity to low intensity (MacInnes and Bracco, 1992). Such an artificial turbulence transfer can be overcome by using the local turbulence at the particle position, instead of being fixed during the particle-eddy interaction time. The normalized fluctuating velocities, determined at the beginning of a particle-eddy encounter, are multiplied by the local turbulence intensity. As a result, the effects of fluid turbulence inhomogeneity on particle dispersion can be accounted for.

Particle inertia

The GI model determines the eddy-interaction time, t_{int}, based on a minimum of an eddy lifetime t_e and an eddy-transit time t_c, which are determined as:

$$t_e = l_e\left(\frac{k}{\varepsilon}\right)^{-1/2}, t_c = -\tau_p \ln\left(1 - \frac{l_e}{\tau_p V_{rel}}\right)(l_e < \tau_p V_{rel}) \tag{19}$$

where the eddy length is given by

$$l_e = C_\mu^{3/4}\frac{k^{3/2}}{\varepsilon} \tag{20}$$

If $l_e > \tau_p V_{rel}$, the particle is trapped by an eddy. As a result, the eddy-interaction time is determined solely by the eddy lifetime. Determined in this way, the eddy-interaction time will cause the heavy particles always to disperse less than the fluid particles in the longtime limit. To take into account that the heavy particles may disperse faster than tracer particles in the longtime limit, Graham and James (1996) suggested that the eddy-interaction time t_{int} of the GI model be modified as follows:

$$t_{\text{int}} = \begin{cases} 2t_e & if\ \ V_{rel} < \frac{2l_e}{\tau_p} \\ \min(T_{\max},\ t_c) & \text{otherwise} \end{cases} \tag{21}$$

where the eddy lifetime t_e is multiplied by a factor of two to ensure that the Lagrangian integral time scales of the actual and model turbulence are consistent. Similarly, the multiplying factor of two for the eddy length scale is aimed at ensuring that the longitudinal scales of the actual and model turbulence are equal. The eddy-transit time t_c in equation (21) is determined in the same way as in equation (19), except that the doubled eddy length is used there. The maximum interaction time $T_{\max}$ is set equal to a value larger than $2t_e$. This will ensure that the heavy particles can disperse faster than the fluid particles. In the present work, $T_{\max} = 3.16t_e$ based upon the analysis (Graham and James, 1996) for a turbulence structure parameter of unity.

Particle-drift correction

It has been found (Adeniji-Fashola and Chen, 1990; Chen and Pereira, 1996) that, for axisymmetric flows, particles tend to accumulate along the centerline downstream; as a result, the particle concentration or mass flux is much overpredicted near the centerline downstream. In the present work, a drift-correction model (Chen and Pereira, 1996) is used, which is aimed at dispersing the particles away from the centerline downstream. The random variable for the component of the radial velocity is modified as:

$$\zeta_v'' = \zeta_v' + \frac{\overline{v^2}}{r_p}\tau_p\alpha_p \tag{22}$$

where r_p is the radial coordinate of the particle position, and α_p is a control parameter to switch on or off the modification; see Chen and Pereira (1996) for details. It is evident that such a modification is only important as the particle is moving close to the centerline ($r_p \rightarrow 0$).

Two-way coupling sources

For a representative particle class k, the momentum-coupling source between the two phases can be derived by integrating the drag force as follows (Durst *et al.*, 1984)

$$\tilde{S}^p_{U_i} = -\frac{1}{\forall}\dot{N}_k \rho \frac{A_p}{2} \int_{t_{in}}^{t_{out}} C_D\left(\tilde{U}_i - U_{pi}\right) V_{rel} dt \tag{23}$$

where A_p is the projection area of a spherical particle, equal to $\pi D_p^2/4$, and t_{in} and t_{out} are the times when the particle enters and leaves the control volume $\forall$. With resort to the particle momentum equations, equation (23) can be rewritten in such a way that the drag force is replaced by the remaining part of the particle momentum equation. As a result, the final source term for all the particles crossing the control volume can be determined as:

$$S^p_{U_i} = \sum \tilde{S}^p_{U_i} = -\frac{1}{\forall}\sum \dot{N}_k \left(\Delta U_{pi} - F_{pi}\Delta t\right)\frac{1}{6}\pi \rho_p D^3_{pi} \tag{24}$$

where $\forall$ is a Eulerian control volume, ΔU_{pi} the particle velocity change when passing through the control volume $\forall$ within the time interval $\Delta t = t_{out} - t_{in}$, and the summation made over all particle trajectories across the control volume $\forall$. Note that F_{pi} in the above equation represents all the forces other than the drag force. With the momentum source determined, the coupling source for the turbulent kinetic energy can be straightforwardly determined by following the same way as the k-equation is derived. The final expression is given by

$$S^p_k = \left\langle \tilde{U}_i \tilde{S}^p_{U_i} \right\rangle - U_i S^p_{U_i} \tag{25}$$

where $\langle\rangle$ denotes realizations over a large number of particles crossing the control volume. The extra dissipation due to the particulate flow is modeled by introducing a model constant $C_{p\varepsilon}$ (see the last term of the right-hand side in equation (7)).

Numerical details

The fluid-flow Eulerian equations are solved in accordance with the curvilinear finite-volume approach (Perić, 1985). The initial conditions are specified from experimental data at the inlet. Typical boundary conditions, such as wall-function modifications and zero-gradient outflow conditions (Launder and Spalding, 1974), are used to solve the discretised Eulerian equations. The flow

computational domain consists of 1,000mm in the streamwise direction and 25.5mm in the radial direction. The flow domain is covered with a grid of 121 × 83 nodes in the x- and y-directions, respectively. Compared with the grids of 100 × 71 and 150 × 100 nodes, such a grid was found to give a grid-independent solution for the liquid flow. The initial conditions for the particle phase are also based on the experimental measurements of the profile near the inlet. A total of 20,000 particle trajectories are tracked for Lagrangian computations. Fully elastic rebounding conditions are applied to account for particle-wall interactions (see Chen (1997) for details). Symmetry boundary conditions are exerted along the central axis for both phases. The tracking of discrete particles in curvilinear coordinates requires developing an efficient particle-locating approach to enhance the Lagrangian computational efficiency (Chen, 1997). In the present work, an improved particle-locating approach (Chen and Pereira, 1999) is adopted that can simultaneously perform particle location, source distribution and particle-field interpolation over the Eulerian control volumes crossed by a particle trajectory.

Results and comparison

The present particle dispersion model is used to predict a turbulent liquid diesel flow laden with glass beads in an axisymmetric sudden-expansion pipe. Experimental measurements (Founti and Klipfel, 1994) are available for both the single- and two-phase flows. The measured flow quantities include mean and fluctuating velocities. For the two-phase flow, the particle-loading ratio is 3 percent by volume. The glass particles have a size distribution ranging from 400μm to 520μm, with a mean equal to 450μm. The densities of the glass beads and liquid diesel are, respectively, 2,500kg/m^3 and 830kg/m^3. The kinematic viscosity of the liquid diesel is 5.21cSt. The inner pipe diameters after and before sudden expansion were 51.0mm and 25.5mm, respectively, yielding an expansion ratio of 2:1.

An accurate prediction of a two-phase flow requires that the numerical model work satisfactorily for both the fluid and particulate flows. Therefore, the nonlinear k-ε turbulence closure model is first evaluated for the single-phase liquid flow. The performance of the model predictions is assessed in terms of comparisons between the numerical predictions and the experimental measurements (Founti and Klipfel, 1994). The numerical grids near the inlet are shown in Figure 1(a), where it can be seen that refined grids are placed near the wall and the inlet to capture the steep gradients there. Figure 1(b) shows the streamlines for the flow close to the inlet. Note that numerical calculations were only performed for the half domain based on the axisymmetry assumption. It is seen that the experimental plane of x = 50mm is located within the recirculation zone, and that the plane of x = 300mm far downstream is away from flow recirculation.

Shown in Figure 2 are the predicted and measured radial profiles of the liquid axial mean velocity at six experimental planes. The numerical predictions of the nonlinear k-ε model using the standard and modified model coefficients are compared with one another and with the experimental measurements. Note that the velocity has been normalized with the maximum velocity of U_{max}= 5.2m/s

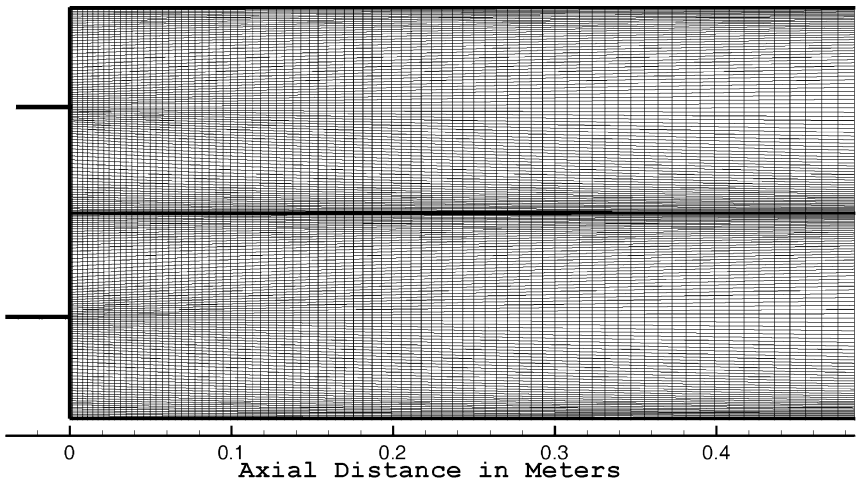

(a)

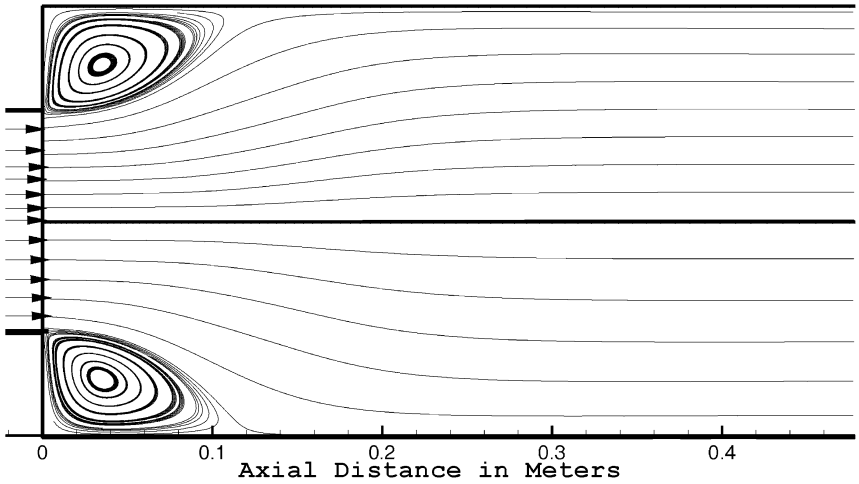

(b)

Figure 1.
Numerical grids (a) and streamlines (b) for the single-phase liquid flow

and that the radial coordinate has been normalized with the large pipe radius R = 25.5mm. It is clear that the numerical predictions are improved with the modified coefficients of C_μ and $C_{\varepsilon 2}$. In contrast, the constant model coefficients have overpredicted the spreading rate downstream of x = 50mm. This is especially true for the three planes of x = 100, 150 and 200mm. The axial mean velocity is slightly underpredicted compared to the experiment.

The predicted and measured radial profiles of the axial and radial RMS velocities are shown, respectively, in Figures 3 and 4 for the six experimental planes. Figures 3 and 4 show that the RMS velocities predicted with the modified model coefficients are generally superior to those predicted with the

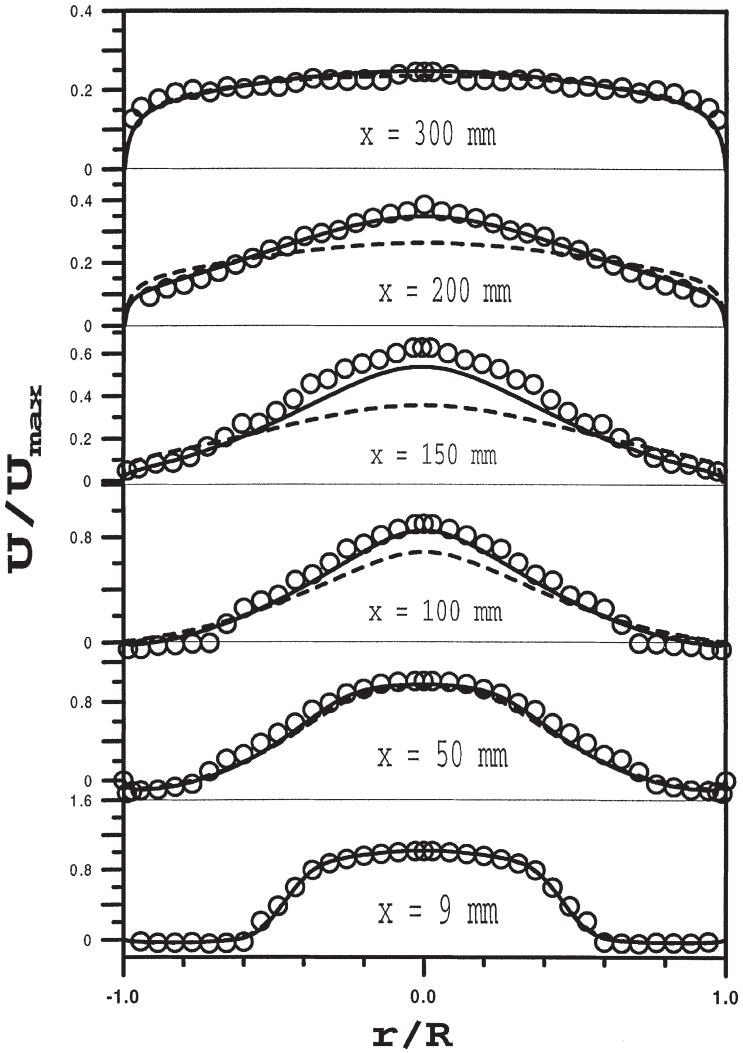

Figure 2.
Profiles of the liquid axial mean velocity ($U_{max} = 5.2$m/s, $R = 25.5$mm)

constant model coefficients. Moreover, it is noted that the nonlinear k-ε model has captured the turbulence anisotropy due to the nonlinear terms in equation (3). This has also been noted in a previous study (Chen and Pereira, 1998). As the flow further develops downstream, the turbulence tends to be isotropic at $x = 300$mm. This can be verified by comparing the two components of the RMS velocity at $x = 300$mm. Figures 2 to 4 have demonstrated that the nonlinear k-ε model should be used in conjunction with the modified model

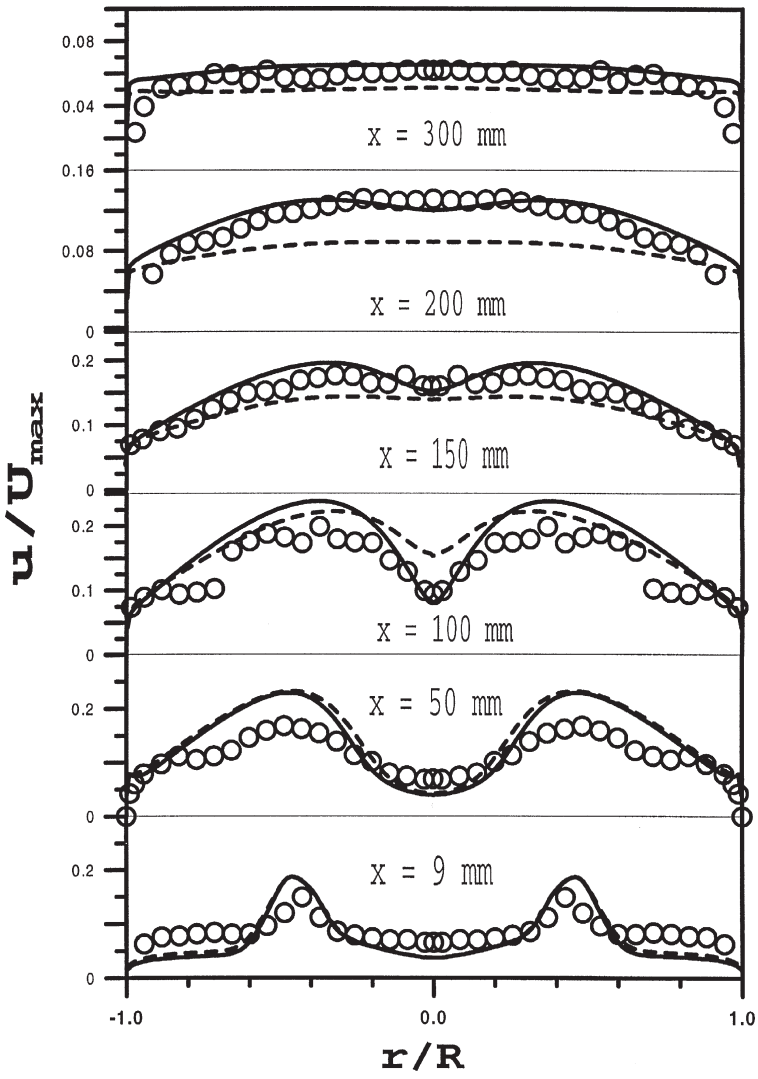

Key:
Symbols: experiment; solid lines, predictions with the modified coefficients; dashed lines, predictions without the modified coefficients

Figure 3.
Profiles of the liquid axial RMS velocity ($U_{max} = 5.2$m/s, $R = 25.5$mm)

coefficients of C_μ and $C_{\varepsilon 2}$, given by equation (10). Hence, the following two-phase calculations are based upon the nonlinear k-ε model using the two modified model coefficients for the turbulent liquid flow.

With the nonlinear k-ε model assessed for the single-phase liquid flow, it is now in a position to validate the hybrid Eulerian-Lagrangian model for two-phase flow predictions. To highlight the difference in model predictions, two

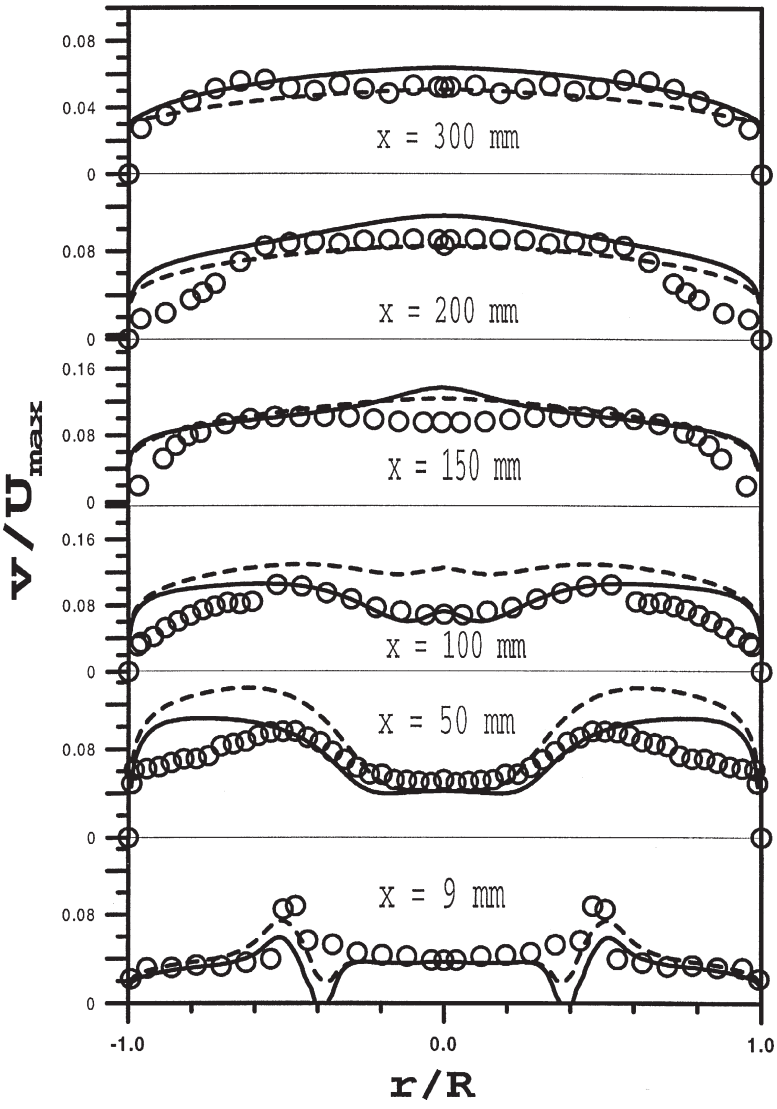

Key:

Symbols: experiment; solid lines, predictions with the modified coefficients; dashed lines, predictions without the modified coefficients

Figure 4.
Profiles of the liquid radial RMS velocity ($U_{max} = 5.2$m/s, $R = 25.5$mm)

representative downstream stations at $x = 50$ and 300mm are chosen for the assessment of two-phase flow predictions. Shown in Figure 5 are the predicted and measured radial profiles of the liquid axial mean velocity for a particle-laden two-phase flow at two downstream stations of $x = 50$ and 300mm,

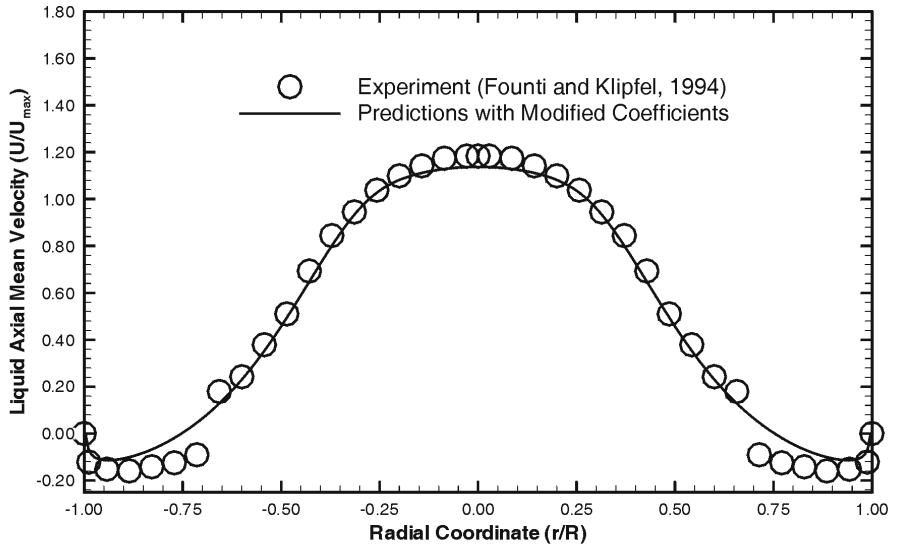

(a) $x = 50\ mm$

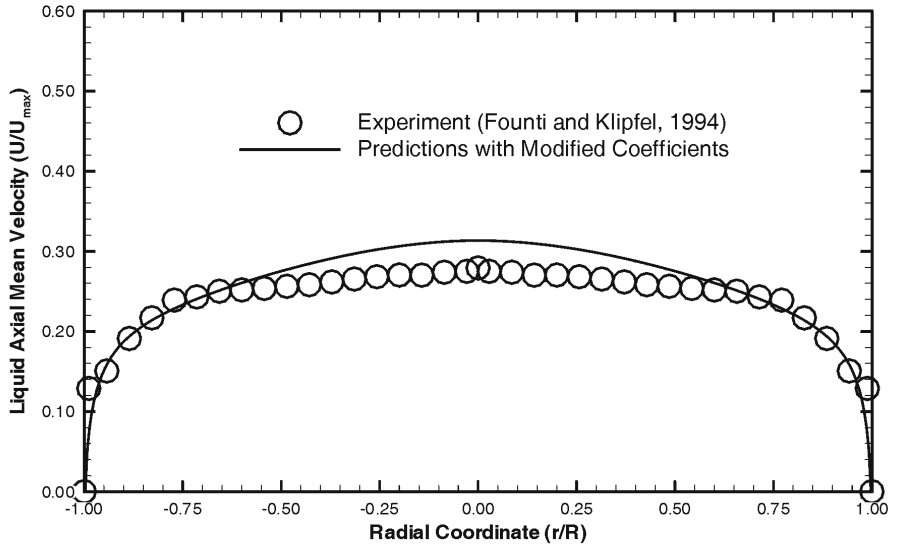

(b) $x = 300\ mm$

Figure 5.
Profiles of the liquid axial mean velocity ($U_{max} = 5.2$m/s, $R = 25.5$mm) for two-phase flow

respectively. Compared with the single-phase flow, the two-phase flow has a slightly higher liquid axial mean velocity at the inlet. It can be seen that the numerical predictions agree very satisfactorily with the experimental measurements. To evaluate the present particle dispersion model for the particulate-phase flow, the predicted and measured radial profiles of the particle axial mean velocity are displayed in Figure 6 for downstream stations

of x = 50 and 300mm, respectively. The predictions with and without the added mass and lift force are also juxtaposed in the figures. In addition, the numerical predictions obtained with the conventional particle dispersion (GI) model are also shown in the Figures for comparison. It is evident that the added mass, lift force and particle dispersion models all have negligible effects on the

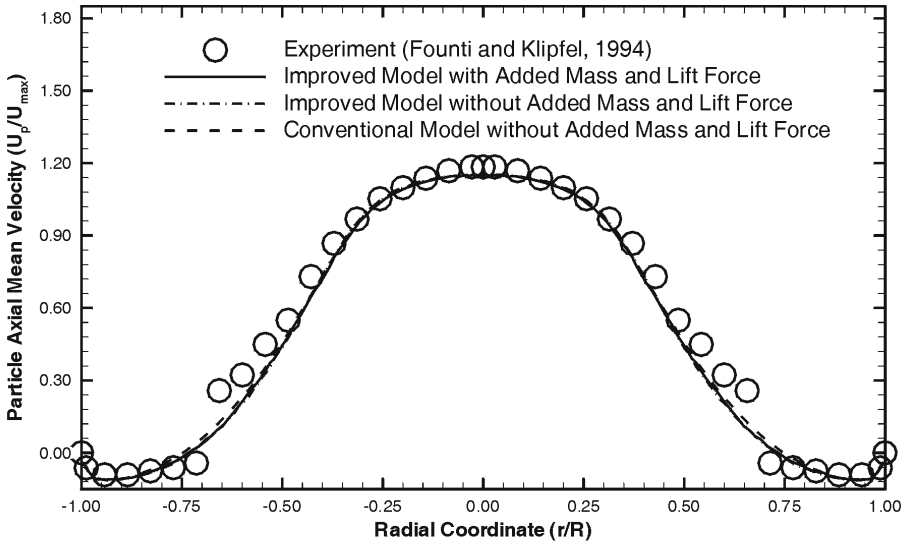

(a) x = 50 *mm*

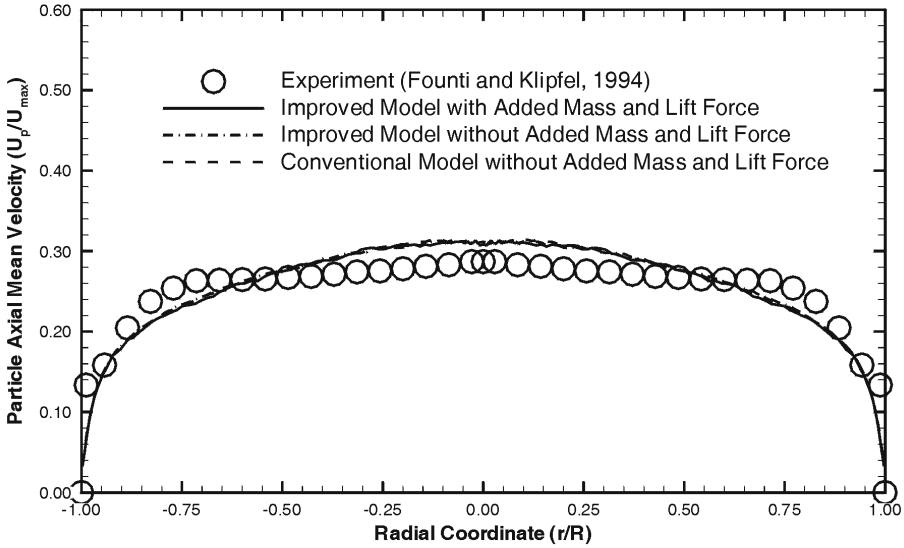

(b) x = 300 *mm*

Figure 6.
Profiles of the particle axial mean velocity ($U_{max} = 5.2$m/s, $R = 25.5$mm) for two-phase flow

particle axial mean velocity; there are no distinguished discrepancies between these model predictions. This suggests that the particle mean flow property is not sensitive to these factors.

The radial profiles of the particle RMS velocities are compared with those measured by Founti and Klipfel (1994) in Figures 7 and 8 for the axial and radial

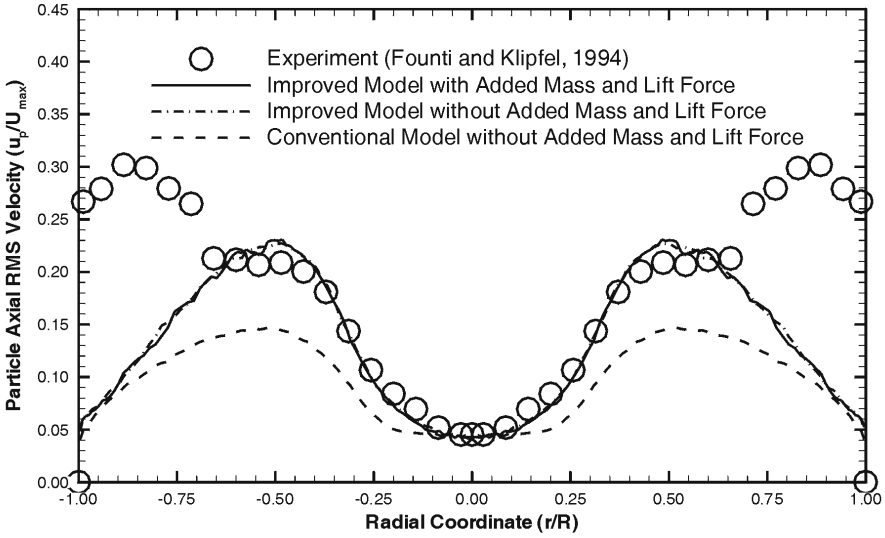

(a) $x = 50\ mm$

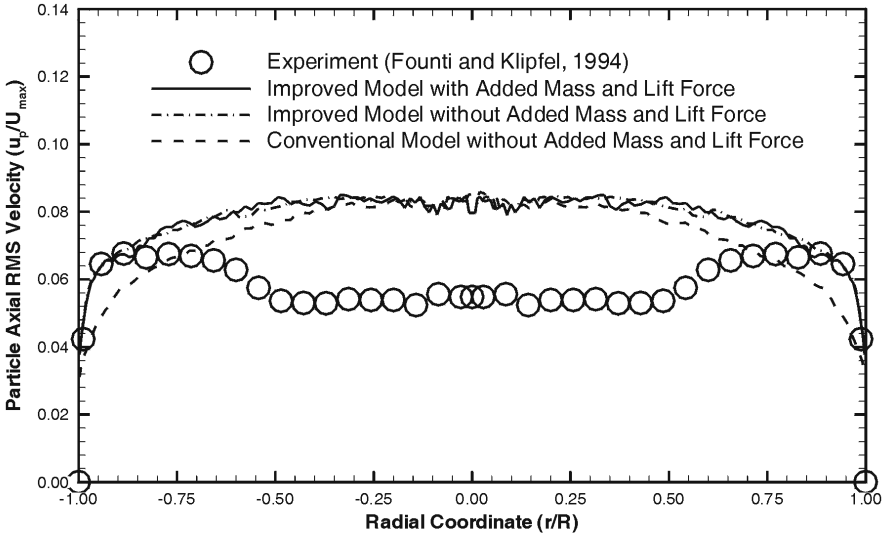

(b) $x = 300\ mm$

Figure 7.
Profiles of the particle axial RMS velocity ($U_{max} = 5.2$m/s, $R = 25.5$mm) for two-phase flow

components, respectively. Again, the two profiles at $x = 50$mm and 300mm are presented and are representative of the flow close to and away from the inlet. Once again, the predictions are not very sensitive to the added mass and the lift force. However, the predictions are very sensitive to the particle dispersion models used. Compared with the original GI model, the improved particle dispersion model (Chen, 2000) has generally ameliorated the prediction of the

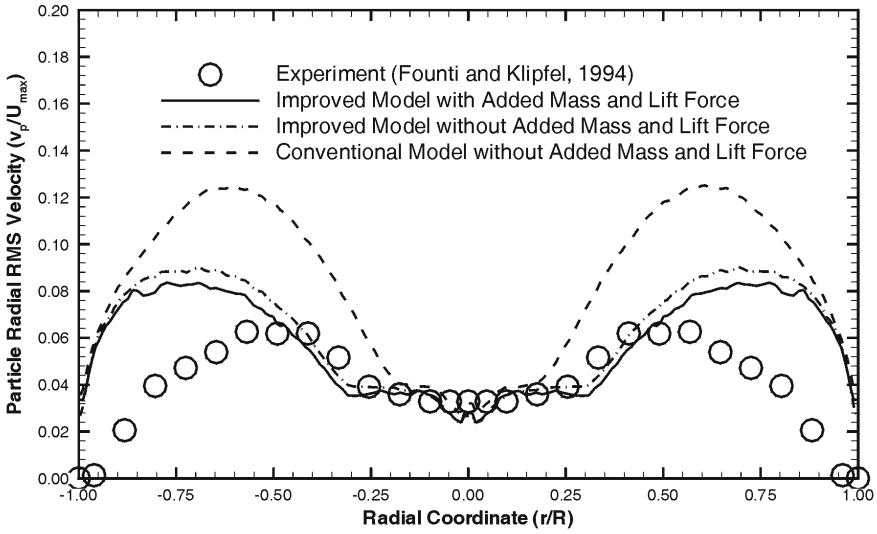

(a) $x = 50\ mm$

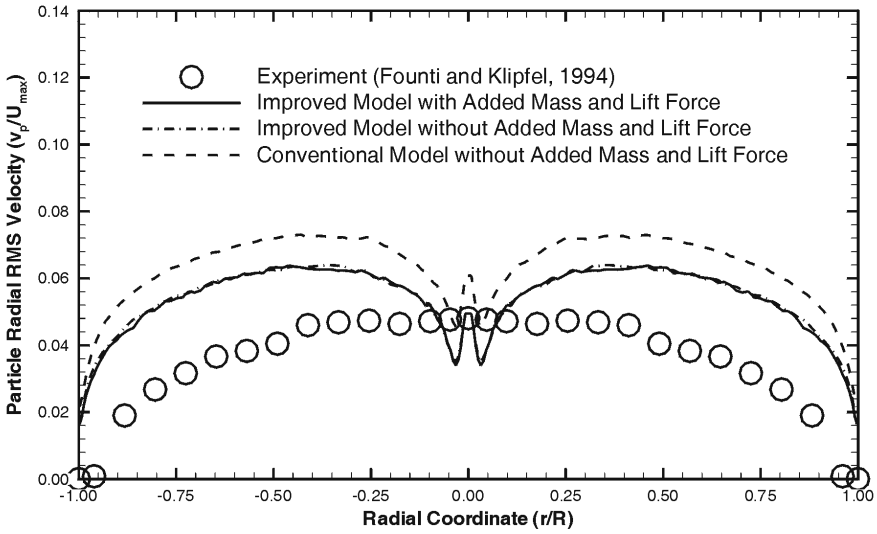

(b) $x = 300\ mm$

Figure 8.
Profiles of the particle radial RMS velocity ($U_{\max} = 5.2$m/s, $R = 25.5$mm) for two-phase flow

particle RMS velocity. Of particular note is that the improved particle dispersion model can adequately account for the effect of turbulence anisotropy. On the contrary, the original particle dispersion (GI) model has almost isotropically predicted the two components of the particle RMS velocities. It is noted that some oscillations are present in the profiles of the radial RMS velocity (see Figure 8(b)). This is attributed to the particle drift-correction model (Chen and Pereira, 1996) used for improving mass-flux predictions. It has been found (Adeniji-Fashola and Chen, 1990; Chen and Pereira, 1996) that, in axisymmetric flows, particles tend to accumulate unrealistically along the centerline further downstream. This is probably due to the fact that the particle radial mean velocity is very small near the centerline far downstream. It is difficult for those particles moving to the region near the centerline to escape from there. A particle-drift correction model (Chen and Pereira, 1996) has to be used to achieve a physically reasonable distribution of particles near the centerline. Figure 8 has shown that better agreement with the experimental measurements is achieved with the improved particle dispersion model (Chen, 2000), even though the two models have underpredicted the particle radial fluctuating velocity.

To study the effects of the two-way coupling sources on the two-phase flow predictions, the numerical predictions including and excluding the source terms in the fluid-flow equations are compared in Figure 9 for the liquid axial mean and RMS velocities at $x = 50$mm, respectively. It is shown that the liquid flow is slightly affected by the coupling source terms as a result of diluteness. Figure 10 shows the particle axial mean and RMS velocities obtained with and without the coupling sources. Once again, slight discrepancies are observed in the two predictions.

Finally, the effects of the shear stress on the particle predictions are compared with the experimental measurements in Figure 11, where the predictions with the random variables correlated, i.e. equation (17), refer to the predictions accounting for the shear stress on the particle dispersion. It is clear that, for the present two-phase flow, the effects of the shear stress are negligible, except for the edge region where the improved predictions accounting for the shear stress are achieved (see Figure 11(b)). It should be noted that some large discrepancies occur in the region near the wall for the plane of $x = 50$mm. This may be attributed either to the model deficiency or to experimental errors. As shown in Figure 1(b), the plane of $x = 50$mm is located within the recirculation region. Only those large particles can penetrate the recirculation zone. It is expected that relatively few particles would penetrate the zone. Therefore, a statistically insufficient number of particles may happen to ensemble averaging for either the experiment or the calculation.

Concluding remarks

A combined Eulerian-Lagrangian model was used to study solid particle dispersion in a turbulent liquid flow. A nonlinear k-ε model was used for the turbulent liquid flow to account for the anisotropy of turbulence. The effects of turbulence anisotropy, turbulence inhomogeneity, particle-drift correction and

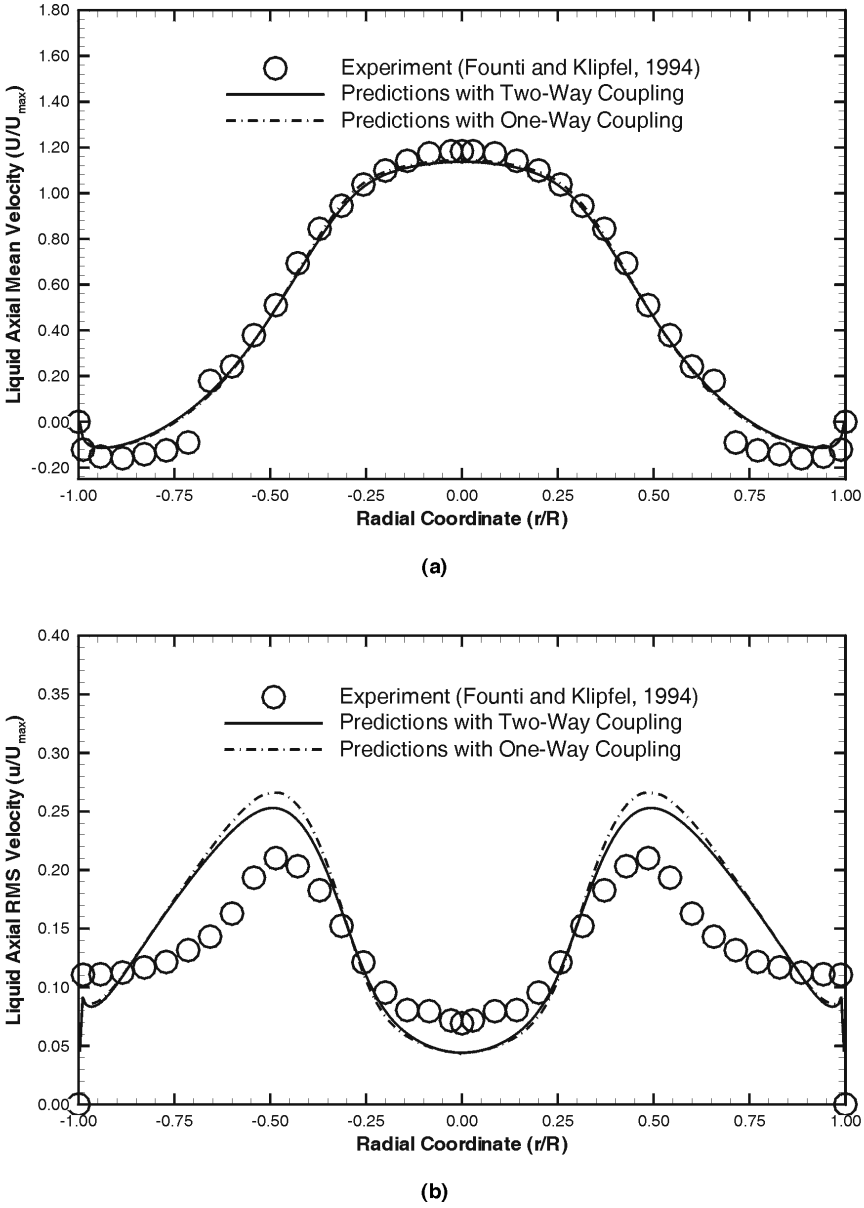

Figure 9.
Effects of the coupling sources on the predicted gas axial (a) mean and (b) RMS velocities x = 50mm ($U_{max} = 5.2$m/s, $R = 25.5$mm) for two-phase flow

particle inertia on particle dispersion are accounted for using an improved eddy-interaction model. The numerical results for both the single-phase and two-phase flows were compared with the corresponding experimental measurements. The effects of the added mass, lift force and shear stress were separately studied. It was found that the modified model coefficients for the fluid flow can achieve better predictions as compared to the experimental

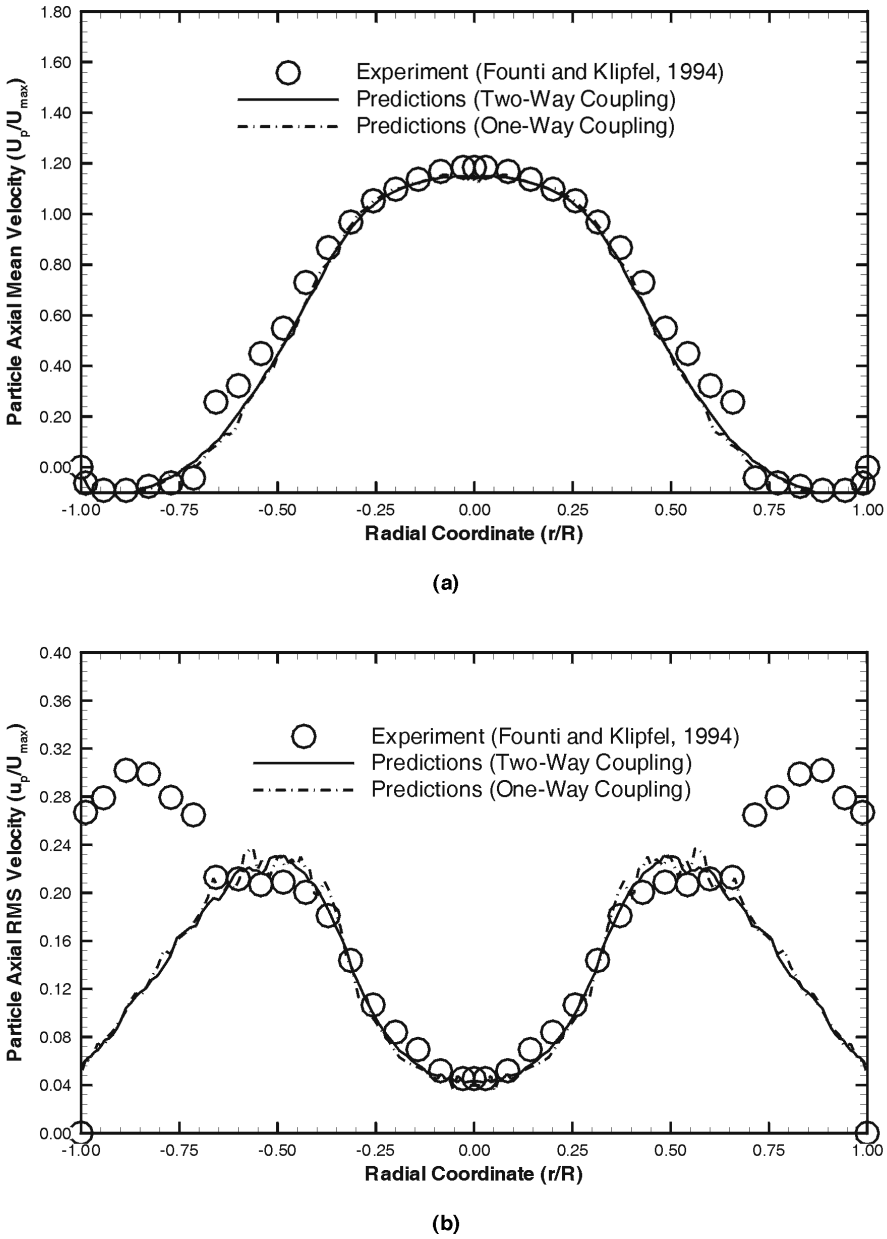

Figure 10.
Effects of the coupling sources on the predicted particle axial (a) mean and (b) RMS velocities x = 50mm ($U_{max} = 5.2$m/s, $R = 25.5$mm)

measurements, that the improved eddy-interaction model has better predicted the anisotropy of particle turbulence than the original GI model, and that the effects of coupling sources, added mass, lift force and shear stress are relatively

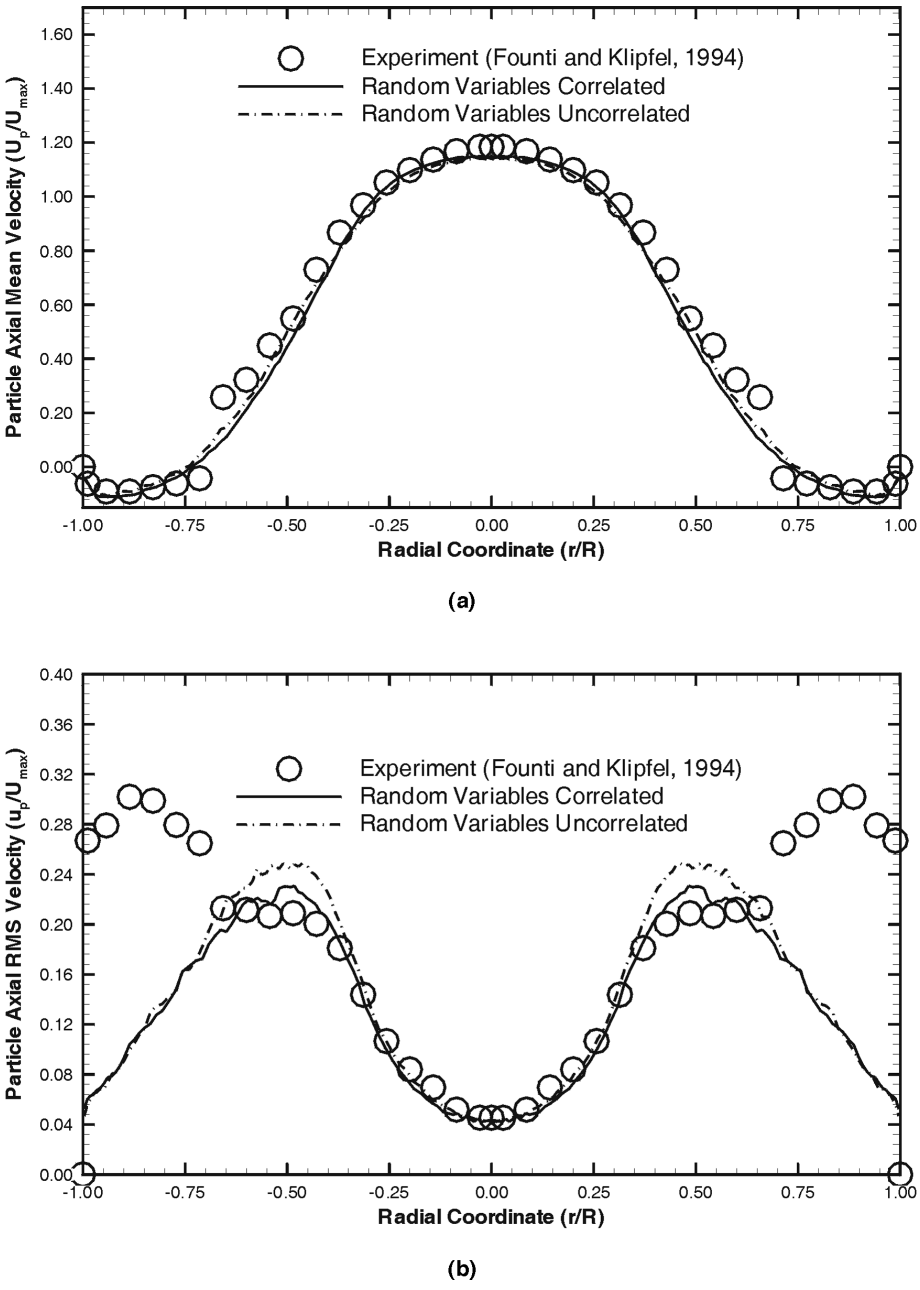

Figure 11.
Effects of the shear stress on the predicted particle axial (a) mean and (b) RMS velocities $x = 50$mm ($U_{max} = 5.2$m/s, $R = 25.5$mm) for two-phase flow

negligible compared to the particle dispersion model. Therefore, the turbulence anisotropy should be accounted for when predicting anisotropic turbulent two-phase flows.

References

Adeniji-Fashola, A. and Chen, C.P. (1990), "Modeling of confined turbulent fluid-particle flows using Eulerian and Lagrangian schemes", *Int. J. Heat Mass Transfer*, Vol. 33, pp. 691-701.

Apsley, D.D. and Leschziner, M.A. (1998), "A new low-Reynolds-number nonlinear two-equation turbulence model for complex flows", *Int. J. Heat Fluid Flow*, Vol. 19, pp. 209-22.

Chang, K.-C., and Wu, W.-J. (1994), "Sensitivity study on Monte Carlo solution procedure of two-phase turbulent flows", *Num. Heat Transfer A*, Vol. 25, pp. 223-44.

Chen, X.-Q. (1997), "An efficient particle-tracking algorithm for two-phase flows in geometries using curvilinear coordinates", *Num. Heat Transfer A*, Vol. 31, pp. 387-405.

Chen, X.-Q. (2000), "Heavy particle dispersion in anisotropic, inhomogeneous, turbulent gas flows", *Int. J. Multiphase Flow*, Vol. 26, pp. 635-61.

Chen, X.-Q. and Pereira, J. C. F. (1992), "Numerical prediction of evaporating and nonevaporating fuel sprays under nonreactive conditions", *At. Sprays*, Vol. 2, pp. 427-443.

Chen, X.-Q. and Pereira, J.C.F. (1996), "Computation of turbulent evaporating sprays with well-specified measurements: a sensitivity study on droplet properties", *Int. J. Heat Mass Transfer,* Vol. 34, pp. 441-54.

Chen, X.-Q. and Pereira, J.C.F. (1998), "Computation of particle-laden turbulent gas flows using two dispersion models", *AIAA J*, Vol. 36, pp. 539-46.

Chen, X.-Q. and J.C.F. Pereira (1999), "A new particle-locating method accounting for source distribution and particle-field interpolation for hybrid modeling of strongly coupled two-phase flows in arbitrary coordinates", *Num. Heat Transfer B*, Vol. 35, pp. 41-63.

Chen, X.-Q., Freek, C. and Pereira, J.C.F. (1996), "Experimental and numerical study of a water spray in the wake of an axisymmetric bluff body", *Experi. Therm. Fluid Sci*., Vol. 13, pp. 129-41.

Chen, X.-Q., Renksizbulut, M. and Li, X. (1999), "A stochastic-probabilistic model for simulation of particle dispersion in general coordinates", *Num. Heat Transfer B*, Vol. 36, pp. 57-82.

Daniel, E. and Loraud, J.-C. (1998), "Numerical simulation of a two-phase dilute flow in a diffuser pipe", *Int. J. Num. Methods Heat & Fluid Flow*, Vol. 8, pp. 224-44.

Durst, F., Milojevic, D. and Schonung, B. (1984), "Eulerian and Lagrangian prediction of particulate two-phase flows: a numerical study", *App. Math. Modeling*, Vol. 8, pp. 101-15.

Founti, M. and Klipfel, A.S. (1994), "Test case specifications –Test Case 1, 7th Workshop on Two-Phase Flow Predictions", April 11-14, Erlangen, Germany.

Gosman, A.D. and Ioannides, E. (1981), "Aspects of computer simulation of liquid-fuelled combustors", AIAA Paper 81-0323.

Graham, D.I. and James, P.W. (1996), "Turbulent dispersion of particles using eddy interaction models", *Int. J. Multiphase Flow*, Vol. 22, pp. 157-75.

Launder, B.E. and Spalding, D.B. (1974), "The numerical computation of turbulent flows", *Comp. Methods App. Mech. Eng.*, Vol. 3, pp. 269-89.

Lien, F.S. and Leschziner, M.A (1994), "Assessment of turbulence-transport models including nonlinear RNG eddy-viscosity formulation and second-moment closure for flow over a backward-facing step", *Comput. Fluids*, Vol. 23, pp. 983-1004.

MacInnes, J.M. and Bracco, F.V. (1992), "Stochastic particle dispersion and the tracer-particle limit", *Phys. Fluids A*, Vol. 4, pp. 2809-24.

Perić, M. (1985), "A finite-volume method for the prediction of three-dimensional fluid flow in complex ducts", PhD thesis, Dept. Mech. Eng., Imperial College, London, UK.

Rodi, W. (1972), "The prediction of free turbulent boundary layers by use of a two-equation model of turbulence", PhD thesis, London University, London.

Sato, Y., Hishida, K. and Maeda, M. (1996), "Effect of dispersed phase on modification of turbulent flow in a wall jet", *J. Fluids Eng.*, Vol. 118, pp. 307-15.